Neuro-Oncology

Establishment of patient-derived organoid models of lower-grade glioma

Kalil G. Abdullah[ORCID]**, Cylaina E. Bird, Joseph D. Buehler, Lauren C. Gattie, Milan R. Savani, Alex C. Sternisha, Yi Xiao, Michael M. Levitt, William H. Hicks, Wenhao Li, Denise M.O. Ramirez, Toral Patel, Tomas Garzon-Muvdi, Samuel Barnett, Gao Zhang, David M. Ashley, Kimmo J. Hatanpaa, Timothy E. Richardson, and Samuel K. McBrayer**

Department of Neurological Surgery, University of Texas Southwestern Medical Center, Dallas, Texas, USA (K.G.A., C.E.B., J.D.B., L.C.G., W.H.H., T.P., T.G.M., S.B.); O'Donnell Brain Institute, University of Texas Southwestern Medical Center, Dallas, Texas, USA (K.G.A., W.L., D.M.O.R., T.P., T.G.M., S.B., K.J.H.); Simmons Comprehensive Cancer Center, University of Texas Southwestern Medical Center, Dallas, Texas, USA (K.G.A., T.P., T.G.M., S.B., S.K.M.); Children's Medical Center Research Institute, University of Texas Southwestern Medical Center, Dallas, Texas, USA (M.R.S., A.C.S., Y.X., M.M.L., S.K.M.); Department of Neurology, University of Texas Southwestern Medical Center, Dallas, Texas, USA (W.L., D.M.O.R.); Duke University School of Medicine, Duke University, Durham, North Carolina, USA (G.Z., D.M.A.); Department of Pathology, Division of Neuropathology, University of Texas Southwestern Medical Center, Dallas, Texas, USA (K.J.H.); Department of Pathology and Laboratory Medicine and The Glenn Biggs Institute for Alzheimer's and Neurodegenerative Diseases, University of Texas Health Science Center at San Antonio, San Antonio, Texas, USA (T.E.R.)

Corresponding Authors: Kalil G. Abdullah, MD, MSc, University of Texas Southwestern Medical Center, 5323 Harry Hines Blvd., Dallas, TX 75390, USA (kalil.abdullah@utsouthwestern.edu); Samuel K. McBrayer, PhD, University of Texas Southwestern Medical Center, 6000 Harry Hines Blvd., Dallas, TX 75390, USA (samuel.mcbrayer@utsouthwestern.edu).

Abstract

Background. Historically, creating patient-derived models of lower-grade glioma (LGG) has been challenging, contributing to few experimental platforms that support laboratory-based investigations of this disease. Although organoid modeling approaches have recently been employed to create in vitro models of high-grade glioma (HGG), it is unknown whether this approach can be successfully applied to LGG.

Methods. In this study, we developed an optimized protocol for the establishment of organoids from LGG primary tissue samples by utilizing physiologic (5%) oxygenation conditions and employed it to produce the first known suite of these models. To assess their fidelity, we surveyed key biological features of patient-derived organoids using metabolic, genomic, histologic, and lineage marker gene expression assays.

Results. Organoid models were created with a success rate of 91% ($n = 20/22$) from primary tumor samples across glioma histological subtypes and tumor grades (WHO Grades 1–4), and a success rate of 87% (13/15) for WHO Grade 1–3 tumors. Patient-derived organoids recapitulated stemness, proliferative, and tumor-stromal composition profiles of their respective parental tumor specimens. Cytoarchitectural, mutational, and metabolic traits of parental tumors were also conserved. Importantly, LGG organoids were maintained in vitro for weeks to months and reanimated after biobanking without loss of integrity.

Conclusions. We report an efficient method for producing faithful in vitro models of LGG. New experimental platforms generated through this approach are well positioned to support preclinical studies of this disease, particularly those related to tumor immunology, tumor-stroma interactions, identification of novel drug targets, and personalized assessments of treatment response profiles.

Key Points

- Organoid models can be efficiently created from LGG tissue samples.
- LGG organoids can be cultured for weeks to months and frozen and reanimated.
- LGG organoids recapitulate parental tumor characteristics.

Importance of the Study

Despite widespread efforts to create cell lines from LGG primary samples, few in vitro models exist to support basic and translational research aimed at combating this disease. Therefore, we optimized a method to derive organoids from primary LGG tissue samples and culture them in vitro. Importantly, organoids maintained molecular and histological characteristics of the primary tumors from which they were established. Our findings outline a novel approach to produce in vitro models of LGG, thereby directly addressing a longstanding challenge in neuro-oncology research. Beyond the fact that they can be created more efficiently than cell line models, LGG organoids also preserve the diverse cellular milieu of these tumors, thereby enabling future studies of the glioma microenvironment.

High-grade gliomas (HGG) are the most common primary malignant tumors of the brain and portend a 5-year survival rate of less than 5%.[1] These tumors may arise de novo as IDH-wildtype glioblastomas (GBMs) or develop from certain progressive lower-grade gliomas (LGGs; defined as WHO Grades 2–3).[2] Despite advances in our collective understanding of glioma pathogenesis, the standard of care regimen of surgical resection followed by temozolomide and radiation has not been modified in over 15 years.[3] The inability to accurately and faithfully model LGG is a major factor contributing to the lack of progress in developing effective new brain tumor therapies. Specifically, there is a paucity of tractable in vitro models of LGG that can be used to support preclinical target identification and drug sensitivity studies. In contrast to the success rates associated with production of HGG cell lines from GBM tissue samples, in vitro models of LGG have proven much more difficult to generate. Virtually all LGG cell lines created to date from adult patients represent oligodendrogliomas, WHO Grade 3,[4–9] thus impeding studies of LGGs in the laboratory. Given the distinct genetic landscape of LGG, in which *IDH1*, *IDH2*, *CIC*, and *ATRX* mutations, as well as co-deletion of 1p/19q chromosome arms, are prevalent, advances in glioma modeling techniques could yield important insights into how these genetic alterations promote gliomagenesis and shape treatment responses.

The application of organoid modeling to neuro-oncology research has provided a new approach to creating models of HGG.[10] Organoid models offer a compelling alternative to traditional cancer cell line or mouse models because they maintain the diverse cell populations observed in murine tumors while supporting higher throughput studies enabled by cell lines. In general, cancer organoids are small (100–500 μm in diameter) tissue spheroids induced from progenitor cells or processed from tumor resections.[11,12] Notably, Jacob et al.[13] recently reported >90% overall success rate in generating in vitro-propagated organoids from HGG tissue samples taken directly from the operating room without adulteration. These organoid cultures accurately recapitulated parental tumor features and treatment response patterns. Moreover, HGG organoids reproduced the complex cellular composition and intratumoral heterogeneity of human gliomas, thereby reflecting a key aspect of glioma biology that is poorly represented in HGG cell lines. Although this study focused exclusively on the production of HGG organoids, this advance in modeling capability suggested that adaptations of the methodology could enable efficient modeling of LGGs.

Drawing on work from other groups,[14–17] we previously found that reducing oxygen tension to 5% (a level reported to be physiologically relevant for brain tissues[18]) facilitated generation of LGG neurosphere cell lines from a genetically engineered mouse model of astrocytoma, IDH-mutant, Grade 3.[19] Therefore, we hypothesized that modifying the method described by Jacob and colleagues to incorporate organoid establishment under conditions closer to physiological oxygenation can be employed to efficiently create patient-derived LGG organoid models. In this study, we collected a series of 22 tissue specimens from glioma resection surgeries, including 15 LGG samples, to directly test this hypothesis. Herein, we demonstrate that explanted LGG organoids are viable and maintain parental tumor characteristics, including cytoarchitecture, cellular heterogeneity, proliferative capacity, and distinctive genomic alterations.

Methods

Additional information can be found in Supplementary Methods.

Human Subjects

Patient tissue and blood were collected following ethical and technical guidelines on the use of human samples for biomedical research at University of Texas Southwestern Medical Center after informed patient consent under a protocol approved by the University of Texas Southwestern Medical Center's Institutional Review Board. All patient samples and organoids were diagnosed and graded according to the 2021 *WHO Classification of Tumours of the Central Nervous System (CNS)*, 5th edition.[20]

Orthotopic Xenograft Glioma Model

All care and treatment of experimental animals were carried out in strict accordance with Good Animal Practice as defined by the US Office of Laboratory Animal Welfare and approved by the University of Texas Southwestern Medical Center's Institutional Animal Care and Use Committee (protocol 2019-102795). MGG152 cells were kindly provided by Drs. Daniel Cahill and Hiroaki Wakimoto (MGH). Cells were implanted orthotopically into ICR SCID mice (Taconic). Upon xenograft establishment, mice were euthanized for brain tissue collection.

Organoid Creation, Culture, and Biobanking

Tumor tissue was collected from the operating room, suspended in ice cold Hibernate A (BrainBits HA), and brought to the lab on ice within 30 minutes from explantation. Tumor pieces were moved into RBC lysis buffer (ThermoFisher 00433357) and incubated at room temperature for 10 minutes with rocking. Next, the tumor pieces were washed with Hibernate A containing Glutamax (final conc. = 2 mM, ThermoFisher 35050061), penicillin/streptomycin (final conc. = 100 U/mL and 100 µg/mL, respectively, ThermoFisher 15140122), and Amphotericin B (final conc. = 0.25 µg/mL, Gemini Bio-Products 400104). Tissues were cut using dissection scissors into 1–2 mm³ pieces and suspended in 1 mL Short-Term Glioma Organoid Medium (formulation provided in Supplementary Methods). One organoid in 1 mL Short-Term Glioma Organoid Medium was plated per well of a 24-well ultra-low adherence plate. Plates were rotated at 120 rpm in a humidified incubator at 37°C, 5% CO_2, and 21% oxygen (Figure 3E) or 5% oxygen (all other figures). Short-Term Glioma Organoid Medium was refreshed in organoid cultures every 48 hours. To freeze, organoids were grouped up to six per well in Short-Term Glioma Organoid Medium containing the ROCK inhibitor Y-27632 (final conc. = 10 µM, Stem Cell Technologies 72302) for 1 hour. Next, DMSO (10% v/v) was added and organoids and media were transferred to a cryotube. They were incubated at 4°C for 15 minutes, frozen at –80°C, and stored long-term in a cryogenic freezer under liquid nitrogen vapor. All organoids presented in the manuscript were cultured for a minimum of four weeks before analysis.

Confocal Microscopy

Fluorescent confocal images were captured on a Zeiss LSM 780 inverted microscope at 10X magnification with tiling. Zen Black software (Zeiss) and ImageJ were used for image capture and analysis, respectively. Organoid viability analysis was performed by staining organoids with Hoechst 33342 and propidium iodide dyes (Ready Probes Kit, ThermoFisher R37610) for 5 minutes in the dark before imaging. Organoid volumes were calculated using the trapezoidal rule using data from live cell image z-stacks of organoids stained with Hoechst 33342.

Histology, Immunohistochemistry, and Immunofluorescence

Organoids were fixed in 10% formalin for 1 hour, washed, and suspended in 70% ethanol. Histology and immunohistochemistry were performed by HistoWiz Inc. (histowiz.com). Immunofluorescence microscopy was conducted by the Whole Brain Microscopy Facility at University of Texas Southwestern Medical Center.

DNA Sequencing and Analysis

DNA was extracted from tissue using the Qiagen DNeasy Blood & Tissue Kit (Qiagen 69504). Library preparation and sequencing were conducted by the University of Texas Southwestern Medical Center Genomics Core facility.

Metabolomics Analysis

Methanolic extracts containing polar metabolites were prepared by disrupting and homogenizing tissues with a TissueLyser II (Qiagen 85300) and tungsten carbide beads (Qiagen 69997). Metabolite extracts were dried under vacuum and reconstituted in 80% Optima acetonitrile (Fisher A955-1) prior to liquid chromatography-mass spectrometry analysis. Metabolite peaks were identified and integrated using El Maven (Elucidata), TraceFinder (ThermoFisher), and FreeStyle (ThermoFisher) software programs. 2-hydroxyglutarate (2HG) levels were compared across samples by calculating the ratio of the 2HG peak area to that of an internal reference metabolite, N-acetyl-asparagine.

Statistics

Statistical analysis was performed with Graphpad Prism (Version 9.0, Graphpad Software, LLC) and included both descriptive statistics as well as tests of statistical significance. For tests of statistical significance involving comparison of two groups, P values were calculated by unpaired t-tests or ratio paired t-tests. For tests of statistical significance involving comparison of three or more groups, P values were calculated by one-way ANOVA tests. For all tests, P values less than .05 were considered to be statistically significant.

Results

Creation of Patient-Derived LGG Organoid Models

To evaluate whether LGG organoid models could be created from primary tissue samples and cultured in vitro under more physiological oxygen levels, we collected 22 specimens from brain tumor resections (Table 1). Resections were conducted via stereotactic, image-guided craniotomy. Tissue samples were parcellated and placed in specialized media and cultured under 5% oxygen with constant rotation. For each glioma from which organoids were created, separate tissue specimens were sent for routine immunohistochemical assessment for pathologic diagnosis. All organoids remained in culture for a minimum of 4 weeks, with a range of 4–24 weeks before processing and analysis.
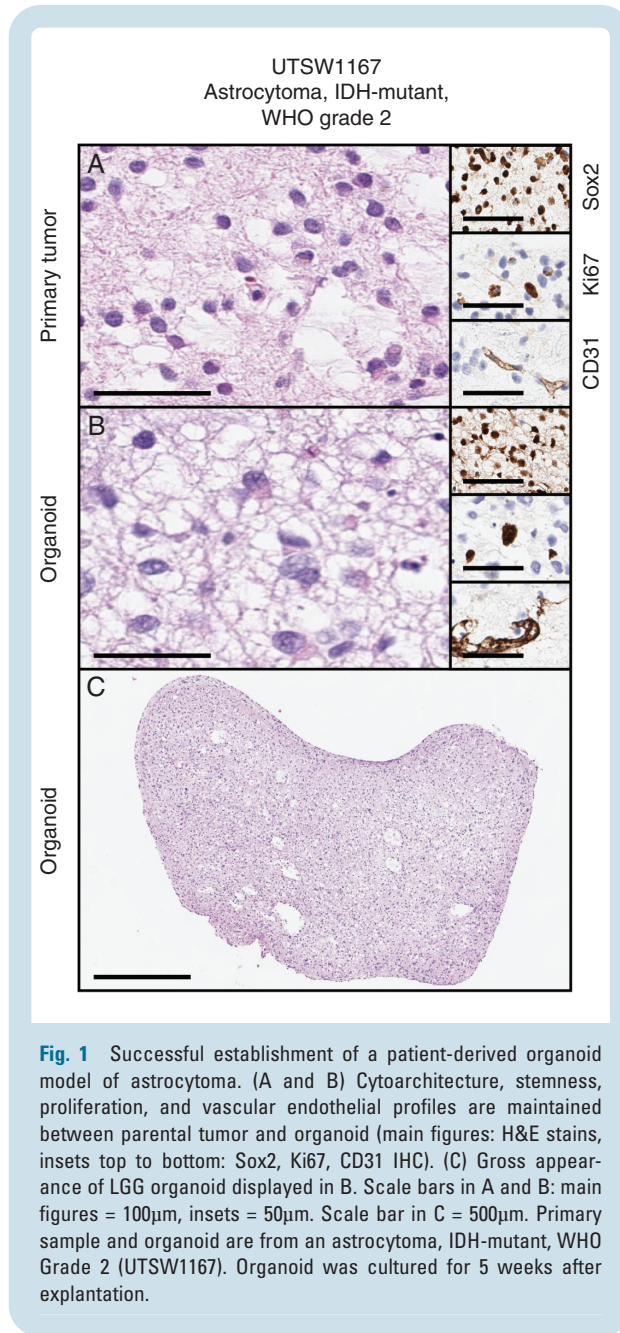
Overall, organoid models were created with a success rate of 91% ($n = 20/22$) from primary tumor samples across glioma histological subtypes and tumor grades (WHO Grades 1–4), and a success rate of 87% (13/15) for WHO Grade 1–3 tumors. We initially performed histological and immunohistochemical evaluation of an organoid model from an astrocytoma, IDH-mutant, WHO Grade 2, and the paired primary tumor specimen from which it was derived. We found that the LGG organoid model recapitulated the histological features of the primary tumor (Figure 1A and B, main figures). Moreover, the organoid model maintained markers of stemness, proliferation, and vascular composition observed in the parent tumor, as assessed by Sox2, Ki67, and CD31 immunohistochemistry (IHC) assays,

Table 1 Organoid and Parental Tumor Characteristics and Demographics

Sample ID	Age	Sex	Brain Region	WHO Grade	Diagnosis	Primary/Recurrent	IDH Mutation	Viable	Tumor DNA	Organoid DNA	Sequenced (weeks)
UTSW2591	55	F	RF	4	GBM, IDH-wildtype	Primary	N/A	Y	Y	Y	4
UTSW1167	38	F	LF	2	Astrocytoma, IDH-mutant	Primary	IDH1 R132H	Y	Y	Y	4
UTSW9534	55	M	RF	3	Astrocytoma, IDH-mutant	Recurrent	IDH1 R132H	Y	N	N	N/A
UTSW8546	42	F	LP	3	Astrocytoma, IDH-mutant	Primary	IDH1 R132S	Y	N	N	N/A
UTSW1164	58	M	LT	4	GBM, IDH-wildtype	Primary	N/A	Y	Y	Y	4
UTSW3968	69	M	LT	3	Astrocytoma, IDH-mutant	Primary	IDH1 R132H	Y	Y	Y	4
UTSW3762	58	M	LP	3	Oligodendroglioma, IDH-mutant, 1p/19q co-deleted	Recurrent	IDH1 R132H	Y	Y	Y	4
UTSW6577	32	M	RP	4	Astrocytoma, IDH-mutant	Recurrent	IDH1 R132H	Y	Y	Y	4
UTSW1382	27	M	LF	3	Oligodendroglioma, IDH-mutant, 1p/19q co-deleted	Recurrent	IDH2 R172K	Y	Y	Y	4
UTSW2243	53	F	LT	4	GBM, IDH-wildtype	Primary	N/A	Y	Y	Y	4
UTSW9647	33	M	RF	3	Astrocytoma, IDH-mutant	Primary	IDH1 R132H	Y	N	N	N/A
UTSW1336	63	F	RF	2	Oligodendroglioma, IDH-mutant, 1p/19q co-deleted	Recurrent	IDH1 R132H	Y	N	N	N/A
UTSW6992	51	M	RF	2	Astrocytoma, IDH-mutant	Primary	IDH1 R132H	Y	N	N	N/A
UTSW3141	44	F	LT	2	Oligodendroglioma, IDH-mutant, 1p/19q co-deleted	Primary	IDH1 R132H	Y	N	N	N/A
UTSW6511	28	F	LT	1	PA	Primary	N/A	Y	N	N	N/A
UTSW2564	73	F	RF	4	GBM, IDH-wildtype	Primary	N/A	Y	Y	N	N/A
UTSW8663	61	F	LF	4	GBM, IDH-wildtype	Recurrent	N/A	Y	Y	N	N/A
UTSW7476	77	F	LT	4	GBM, IDH-wildtype	Primary	N/A	Y	N	N	N/A
UTSW4699	57	M	RF	3	Oligodendroglioma, IDH-mutant, 1p/19q co-deleted	Recurrent	IDH1 R132H	Y	N	N	N/A
UTSW4588	27	M	LP	3	Oligodendroglioma, IDH-mutant, 1p/19q co-deleted	Recurrent	IDH2 R172K	Y	N	N	N/A
UTSW4432	40	M	RF	3	Astrocytoma, IDH-mutant	Primary	IDH1 R132H	N	N	N	N/A
UTSW2933	32	M	RF	3	Astrocytoma, IDH-mutant	Primary	IDH1 R132H	N	N	N	N/A

List of primary tumor specimens and organoid models in the study. "Brain Region" column specifies location of the tumor at resection, abbreviations: RF, right frontal; LF, left frontal; LP, left parietal; RP, right parietal. "Diagnosis" column abbreviations: GBM, glioblastoma; PA, pilocytic astrocytoma. IDH status of each primary tumor sample was assessed via IHC, genomic DNA sequencing, or both. "Tumor DNA" and "Organoid DNA" columns indicate whether sequencing was performed. "Sequenced" column indicates the number of weeks following tumor explantation at which organoids were fixed for sequencing analysis. "Viable" column denotes organoid structural integrity at 4 weeks. UTSW2243 was sequenced but failed to meet quality assurance standards and sequencing results were omitted from further analysis. For all columns, Y = Yes, N = No, N/A = not applicable.

respectively (Figure 1A and B, insets, and Supplementary Figure 1). At a macroscopic level, LGG organoids demon-

UTSW1167
Astrocytoma, IDH-mutant,
WHO grade 2

Fig. 1 Successful establishment of a patient-derived organoid model of astrocytoma. (A and B) Cytoarchitecture, stemness, proliferation, and vascular endothelial profiles are maintained between parental tumor and organoid (main figures: H&E stains, insets top to bottom: Sox2, Ki67, CD31 IHC). (C) Gross appearance of LGG organoid displayed in B. Scale bars in A and B: main figures = 100μm, insets = 50μm. Scale bar in C = 500μm. Primary sample and organoid are from an astrocytoma, IDH-mutant, WHO Grade 2 (UTSW1167). Organoid was cultured for 5 weeks after explantation.

strated demarcated borders and macroscopic hallmarks of analogous primary tumors (Figure 1C). These findings suggested that our organoid-based approach, in contrast to conventional approaches for producing adherent or neurosphere cell line models, may support efficient creation of new patient-derived in vitro models of LGG.

Next, we expanded our assessment of patient-derived organoids across multiple histological subtypes and all grades of glioma. In addition to the astrocytoma, IDH-mutant, WHO Grade 2 model evaluated in Figure 1, we also assessed organoids produced from a pilocytic astrocytoma,

WHO Grade 1, an oligodendroglioma, IDH-mutant, 1p/19q co-deleted, WHO Grade 3, and an astrocytoma, IDH-mutant, WHO Grade 4. We again observed that histological characteristics and cellularity of organoids resembled that of their parental tumors (Figure 2A–L). Importantly, the number of Ki67-expressing cells in glioma organoids correlated positively with tumor grade (Figure 2M–P; Supplementary Figure 2A), demonstrating that features related to glioma aggressiveness and progression are preserved in these in vitro cultures. As an additional validation of organoid integrity, we stained pilocytic astrocytoma and diffuse astrocytoma organoids with dyes marking live and dead cells and found that the vast majority of cells in these cultures were viable (Supplementary Figure 2B and C).

One potential advantage that organoids offer over cell lines is that they can preserve key aspects of the tumor microenvironment. Gliomas contain diverse populations of malignant and stromal cells that have been shown to interact with one another in ways that influence tumor evolution and response to therapy. Therefore, we sought to determine whether stromal cells were maintained in our organoid cultures. Using a dual immunofluorescence (IF) assay, we confirmed the presence of macrophages/microglia (via Iba1 expression) and vascular endothelial cells (via CD31 expression) in organoids (Figure 2Q–X). Macrophage/microglia populations were present in each model evaluated while vascular endothelial cells were selectively observed in the astrocytoma, IDH-mutant, WHO Grade 2 and oligodendroglioma, IDH-mutant, 1p/19q co-deleted, WHO Grade 3 models. Therefore, patient-derived LGG organoids contain a heterogeneous cellular milieu that is characteristic of human brain tumors.

2-Hydroxyglutarate Accumulation is Observed in IDH-Mutant LGG Organoids

Point mutations in *IDH1* and *IDH2* genes are canonical drivers of gliomagenesis[21] and are present in more than 70% of adult LGGs. Mutant IDH enzymes synthesize the oncometabolite 2-hydroxyglutarate (2HG), leading to profound epigenetic and transcriptomic changes in glioma cells.[22,23] Moreover, recent updates to WHO diagnostic categories for adult patients with central nervous system tumors effectively eliminate the diagnosis of IDH-wildtype oligodendroglioma,[20] thereby further solidifying the association between *IDH1/IDH2* mutations and LGG biology. Therefore, we sought to determine if mutant IDH oncoprotein expression and 2HG accumulation persist in IDH-mutant LGG organoids.

We first conducted histological analysis of an organoid produced from an astrocytoma, IDH-mutant, WHO Grade 3 tissue sample that harbored an *IDH1* R132H mutation. We found that the organoid model retained key macroscopic structural features of human gliomas of similar grade, including the presence of a well-defined longitudinal vascular channel that permeated the center of the organoid (Figure 3A, main figure and lower right inset). Next, we performed IHC for the IDH1 R132H mutant enzyme and found that the organoid, like the primary specimen from which it was derived, displayed pervasive oncoprotein expression (Figure 3A, upper right insets). Similar staining patterns
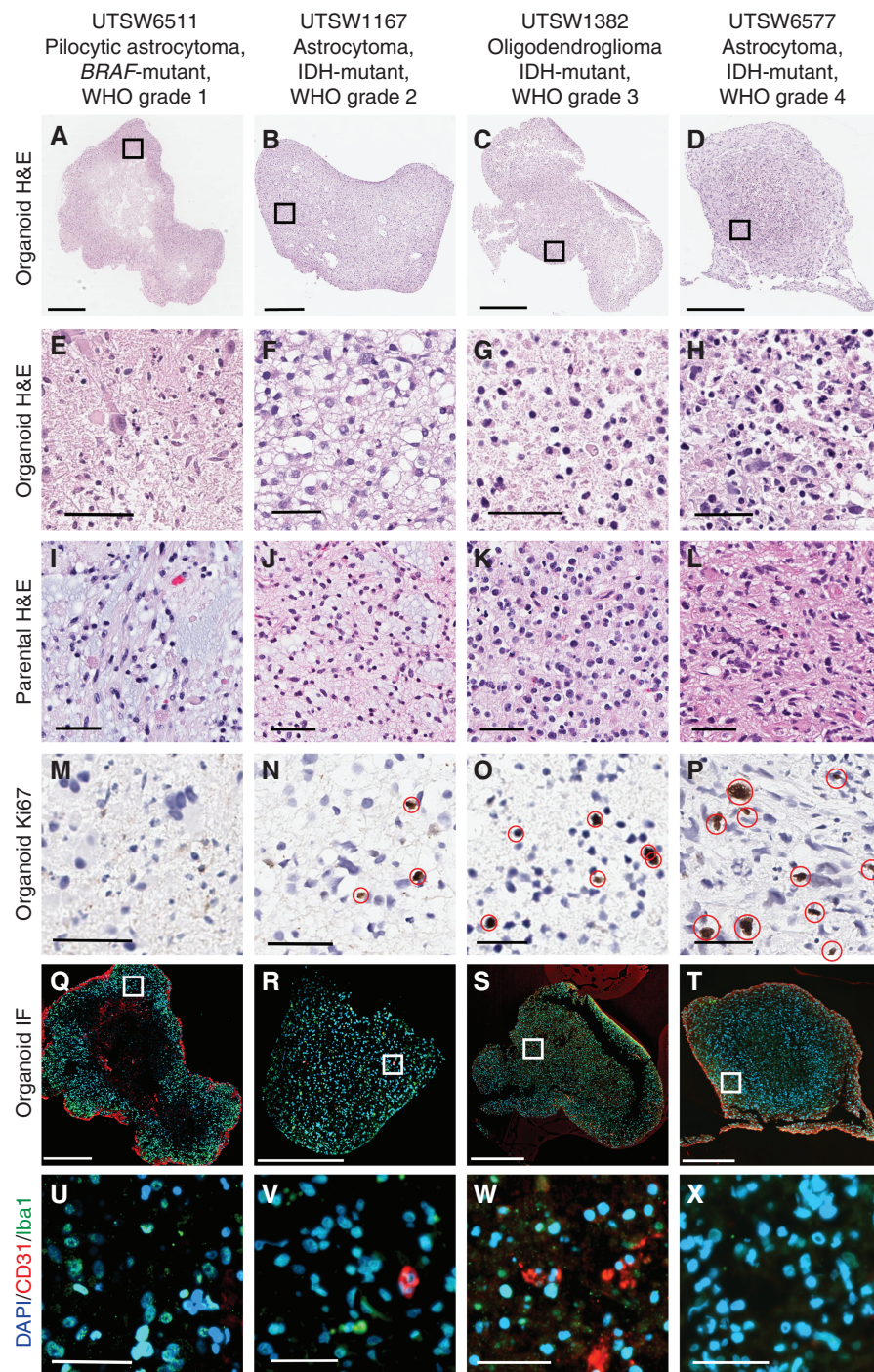
Fig. 2 Glioma organoids recapitulate cellular heterogeneity and parental tumor characteristics across tumor grades. Macroscopic (A–D) and high-powered view (E–H) of organoids and corresponding parental tumors (denoted "parental", I–L) spanning WHO Grades 1–4. (M–P) Cellular proliferation in organoids, as measured by Ki67 IHC, correlates with parental tumor grade. Immunofluorescence microscopy detection of macrophages/microglia and vascular endothelial cells present in organoids at low- (Q–T) and high-powered (U–X) views. Note: CD31 positivity not observed in panels U and X. Red ellipses denote Ki67+ cells. In Q–X, blue = DAPI, red = CD31, green = Iba1. Scale bars: A–D, Q–T = 500 μM, all others = 50 μM. Organoids were cultured for 4–6 weeks after explantation.

were observed in two additional LGG organoid models derived from gliomas positive for the *IDH1* R132H mutation (Figure 3B, upper and middle panels). Importantly, positive and negative staining of tumor and normal brain tissues, respectively, in a patient-derived orthotopic xenograft model of astrocytoma, IDH-mutant, WHO Grade 4[24]
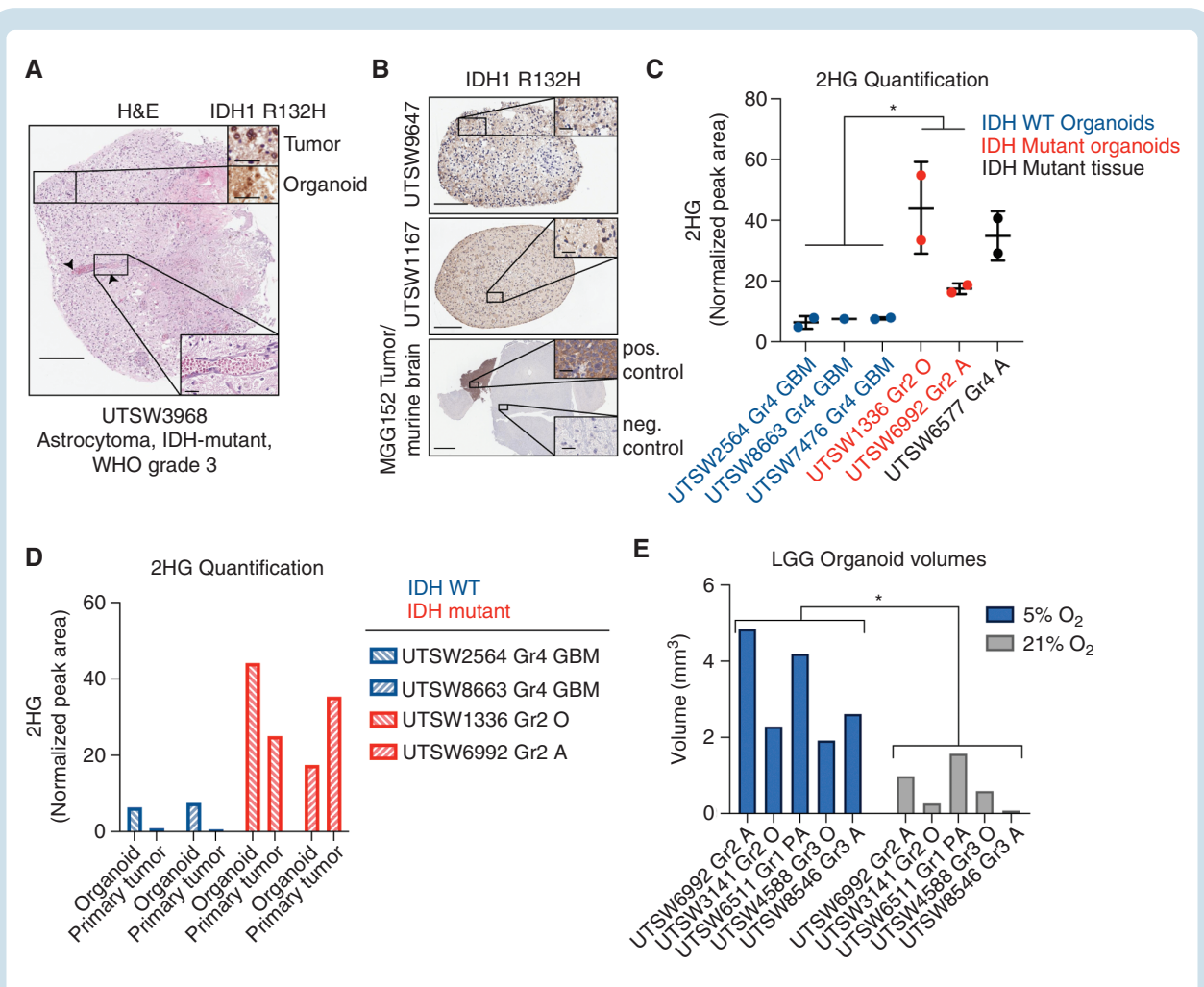
Fig. 3 IDH1 oncoprotein expression and 2HG production are preserved in LGG organoids. (A) Main figure: H&E stain of an organoid derived from an *IDH1* R132H-positive astrocytoma. Arrows denote a longitudinal vascular channel, which is shown at higher magnification in lower inset. Upper insets: IDH1 R132H oncoprotein detection by IHC in primary tumor and organoid tissues. Scale bars: main figure = 250 μm, insets = 50 μm. (B) IDH1 R132H oncoprotein IHC in two astrocytoma organoid models, UTSW9647 and UTSW1167, and in normal and malignant brain tissue in the MGG152 orthotopic xenograft model of astrocytoma, IDH-mutant, WHO Grade 4 (scale bars in main figures = 200 μm, 500 μm, and 2 mm, respectively). Scale bars in insets = 50 μm. Staining patterns in MGG152 tumor tissue and normal murine brain tissue serve as positive and negative controls, respectively. (C) LC-MS-based 2HG quantification in IDH-wildtype organoids (blue), IDH-mutant organoids (red), and an IDH-mutant primary tumor tissue sample (black, positive control). (D) LC-MS-based 2HG quantification in paired organoid and primary tumor tissues from selected specimens in C. Blue = IDH-wildtype, red = IDH-mutant. In parts C and D, values represent 2HG peak areas relative to that of an internal reference metabolite, N-acetyl-asparagine. (E) Organoids were cultured under either 5% (physiologic) or 21% (supraphysiologic) oxygen. Organoid volumes were calculated via microscopy. Abbreviations: Gr, Grade; GBM, glioblastoma; O, oligodendroglioma; A, astrocytoma; PA, pilocytic astrocytoma. In C, data are means ±standard deviation; two-tailed P value was determined by unpaired t-test. In E, two-tailed P value was determined by ratio paired t-test. * $P < .05$. Organoids were cultured for 4–6 weeks after explantation.

affirmed IHC assay specificity (Figure 3B, lower panel). Finally, to test whether 2HG accumulation is observed in organoid models of IDH-mutant LGG, we performed liquid chromatography-mass spectrometry (LC-MS) analysis of metabolite content in a collection of organoids with defined IDH status. As a positive control, we also quantified 2HG in a primary tissue specimen from an astrocytoma, IDH-mutant, WHO Grade 4. We observed elevated levels of 2HG in IDH-mutant, Grade 2 glioma organoids relative to GBM, IDH-wildtype organoids (Figure 3C), and these levels approximated those present in the corresponding parent tumor tissue specimens (Figure 3D). Therefore,

patient-derived organoids preserve a central metabolic hallmark of LGG.

Lower Oxygen Conditions Facilitate LGG Organoid Culture

We hypothesized that more physiological oxygenation may enhance the development of in vitro models of LGG. As such, after our initial success in establishing organoids from an astrocytoma, IDH-mutant, WHO Grade 2 sample under 5% oxygen (Figure 1), we applied a similar

experimental scheme for subsequent organoid cultures. To directly test whether reduced oxygen tension contributed to successful LGG organoid establishment, we prospectively collected a series of primary LGG tissue samples of various grades and cultured them under different oxygen tensions.

We sectioned explanted tissue to similarly sized spheroids (~200 µm in diameter), and incubated spheroids under either physiologic (5%) or high (21%) oxygen tension. After 4 weeks, many LGG organoids incubated under 21% oxygen lost structural integrity and fragmented in culture, thereby precluding an accurate assessment of their volumes. Therefore, we selected representative organoids from those remaining for each model at 5% and 21% oxygen, stained them with Hoechst 33342 and propidium iodide dyes, and performed confocal microscopy to calculate their volumes. We found a marked decrease in organoid volume in organoids grown under 21% oxygen versus 5% oxygen (Figure 3E). The average volume of organoids grown under 5% oxygen was 3.2 mm^3 +/− 1.3 and 0.70 mm^3 +/− 0.60 under 21% oxygen conditions ($P < .05$). Therefore,

conditions closer to physiological oxygenation enhance the establishment of LGG organoids, although reduced oxygen tension is not strictly required. Given this finding, we continued to employ 5% oxygen culture conditions for all subsequent studies.

LGG Organoids Maintain Fidelity During Long-Term Culture and After Biobanking

To determine the impact of prolonged culture in our model system, organoids from an astrocytoma, IDH-mutant, WHO Grade 3 specimen were analyzed after culture for 1 or 6 months. Organoids cultured for 6 months showed similar cytoarchitecture, prevalence of proliferating cells, vascularity, and overall cellularity as those cultured for 1 month post-explantation (Figure 4A–F; Supplementary Figure 3). To assess the capacity of LGG organoids to be biobanked and reanimated to support on-demand experimentation, we used a previously published protocol[13] to assess the effects of cryopreservation on key characteristics of
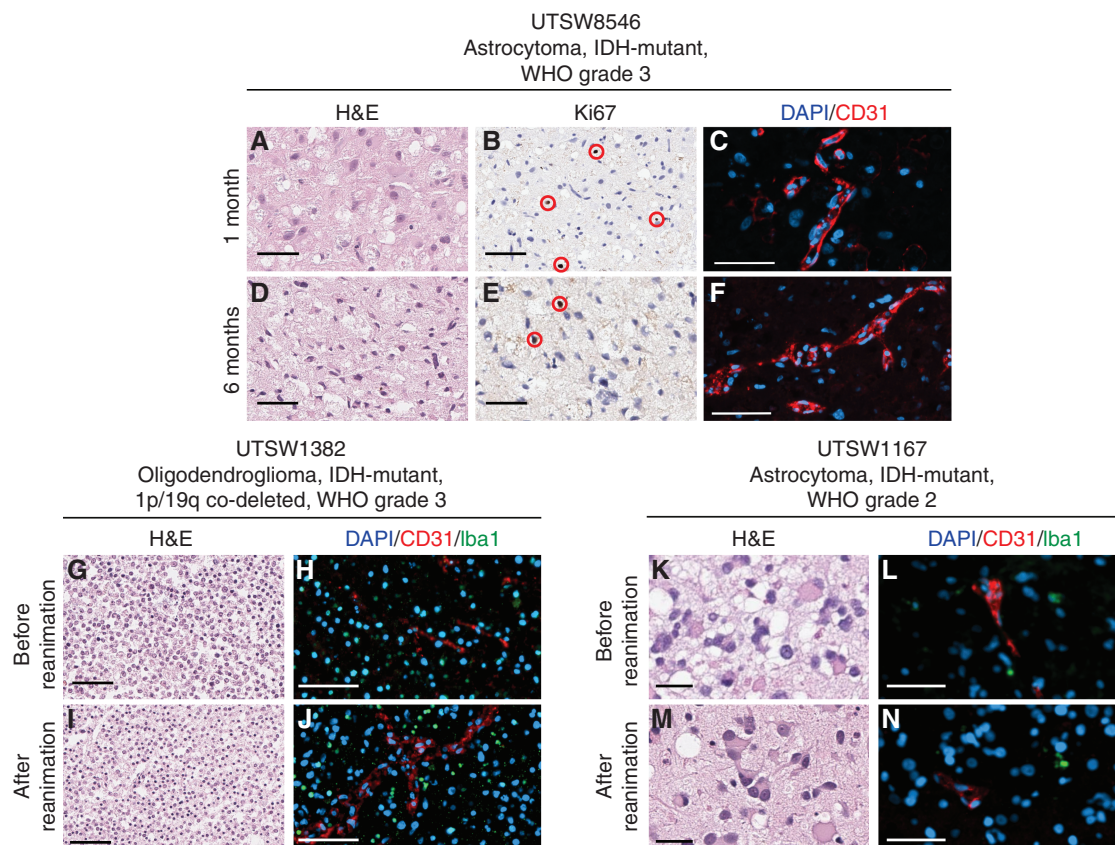
Fig. 4 Organoids maintain cytoarchitecture and proliferation during long-term culture and can be cryopreserved. Organoids from an astrocytoma, IDH-mutant, WHO Grade 3 (USTW8546) were cultured for 1 month (A–C) or 6 months (D–F) prior to analysis. Organoids were evaluated by H&E staining (A and D), Ki67 IHC (B and E), and CD31 IF (C and F). In parts B and E, red ellipses denote Ki67+ cells. Organoids from an oligodendroglioma, IDH-mutant, 1p/19q co-deleted, WHO Grade 3 (UTSW1382) and an astrocytoma, IDH-mutant, WHO Grade 2 (UTSW1167) were cultured for 4 weeks and analyzed immediately (G, H, K, and L) or biobanked, reanimated, and cultured for one week prior to analysis (I, J, M, and N). Organoids were evaluated by H&E staining (G, I, K, and M) and CD31/Iba1 IF (H, J, L, and N). In C, F, H, J, L, and N, red = CD31 and blue = DAPI. In H, J, L, and N, green = Iba1. In G–J, scale bars = 100 µm. In all other panels, scale bars = 50 µm.

organoids established from an oligodendroglioma, IDH-mutant, 1p/19q co-deleted, WHO Grade 3 (Figure 4G–J) and an astrocytoma, IDH-mutant, WHO Grade 2 (Figure 4K–N). We found that organoids that were previously frozen displayed similar cytoarchitecture and composition of diverse cell populations relative to those that were not frozen.

Parental Tumor Genetic Alterations are Preserved in LGG Organoid Models

We showed that patient-derived LGG organoids recapitulate key morphological, metabolic, and cellular features of parental tumor specimens, although their genomic fidelity had not been addressed. To ask if organoids retained genetic hallmarks of LGG, we performed next-generation DNA sequencing on pairs of organoids and parental tissue samples representing 3 HGGs and 4 LGGs using a targeted panel covering 1425 genes. Cancer-associated variant allele frequencies (VAFs) were calculated for genes commonly mutated in LGG, including *IDH1*, *IDH2*, *TP53, NOTCH1*, *NOTCH2*, *CIC*, and *ATRX*, and we observed broad concordance between mutational patterns in LGG organoids and their respective parental tumor samples (Figure 5A). These data are in agreement with our findings that mutant IDH1 oncoprotein expression and 2HG accumulation are preserved in IDH-mutant LGG organoids (Figure 3). We did note moderate variability in VAFs for *CIC*, *NOTCH2*, and *TP53* genes between organoids and primary samples, although it is unclear whether these changes reflected genetic evolution in culture or spatial genetic heterogeneity[25] in the primary tumor. As anticipated, the prevalence of mutations in this suite of genes was much lower in two GBM, IDH-wildtype samples (which were included as references) in relation to LGG and astrocytoma, IDH-mutant, WHO Grade 4 samples.

We also used DNA sequencing data to analyze copy number variation (CNV) in pairs of LGG organoids and primary tissue samples and included a pair of GBM, IDH-wildtype samples for reference (Figure 5B). Copy number losses and gains seen in the primary tumor samples were largely preserved in organoids. Importantly, pathognomonic loss of 1p and 19q segments in oligodendrogliomas was strictly conserved in oligodendroglioma organoids. We did observe sporadic evidence of copy losses or gains of chromosome regions or entire chromosomes that distinguished organoids and primary specimens. However, one LGG sample pair (UTSW1382, oligodendroglioma, IDH-mutant, 1p/19q co-deleted, WHO Grade 3) showed evidence of loss of single copies of chromosomes 13, 14, and 15 only in the primary tumor specimen, suggesting that clonal heterogeneity of the primary tumor contributed to some of the divergence in genomic profiles between paired samples. Collectively, these data demonstrate high genetic fidelity of patient-derived LGG organoid models.

Discussion

Our findings reveal a promising new strategy to produce cell culture models of LGG. This organoid-based modeling approach preserved molecular, cellular, and morphological characteristics of human LGGs during prolonged culture periods and after biobanking. Our strategy builds on a landmark study[13] that detailed highly efficient generation of HGG organoids from surgical specimens. In this study, we sought to optimize and apply a similar methodology to create patient-derived LGG organoids to address the shortage of faithful in vitro models of this disease. Interestingly, Yuan and colleagues recently applied an alternative methodology, conditional reprogramming,[26] to generate cell lines from a number of LGGs, including pediatric pilocytic astrocytoma and ganglioglioma specimens.[27] The conditional reprogramming method, which entails culture in fibroblast-conditioned media supplemented with a Rho kinase inhibitor, was shown to offer a distinct advantage over conventional serum-replete and serum-free culture conditions. In contrast to our study, Yuan and colleagues focused primarily in pediatric LGGs and their method did not yield cell lines from specimens harboring *IDH* mutations, which are more common in adult LGGs. Therefore, our study offers a complementary method tailored to the challenges inherent to establishing adult LGG models that, together with the approach described by Yuan and colleagues, presents compelling opportunities to expand in vitro models of glioma that span histological and age-specific tumor subtypes.

A key feature of our organoid culture method that diverged from the method described by Jacob et al.[13] is the implementation of conditions that more closely approximate physiological oxygenation. Importantly, we found that establishing LGG organoids at 5% oxygen produced larger organoids with greater structural integrity relative to ambient 21% oxygen. These findings are in agreement with our previous observation that more physiological oxygen levels enable the creation of astrocytoma, IDH-mutant, Grade 3 astrocytoma cell lines from a genetically engineered mouse model of this disease.[19] Although the benefits of this approach for generating in vitro models of LGG are clear, understanding why LGG cultures benefit from these lower oxygen conditions will be an important topic to address in future studies. Previous research has shown that HIF2α, but not HIF1α, is preferentially stabilized in glioma stem-like cells grown under 2–5% oxygen.[17] This finding has relevance for our present study because HIF2α and HIF1α appear to exert opposing effects on glioma cell fitness, with HIF2α increasing fitness[16] while HIF1α has been linked to tumor suppression in this context.[5,28] An alternative explanation for the beneficial effects of more physiological oxygenation could be that lower oxygen tensions produce less oxidative stress in cultured cells, which has been noted in a variety of in vitro models.[15] Indeed, we have found that decreased oxygen levels promote resistance to oxidative stress caused by impairments in glutathione metabolism, particularly in glioma cells carrying *IDH1* mutations.[29] Investigating these and other potential mechanisms underlying our findings may reveal LGG-specific vulnerabilities that could be offset for the purposes of disease modeling or exploited for therapeutic intervention.

In addition to propagating LGG tumor cells in culture, the ability to faithfully model the complexity of diffuse gliomas in the laboratory represents a pervasive and
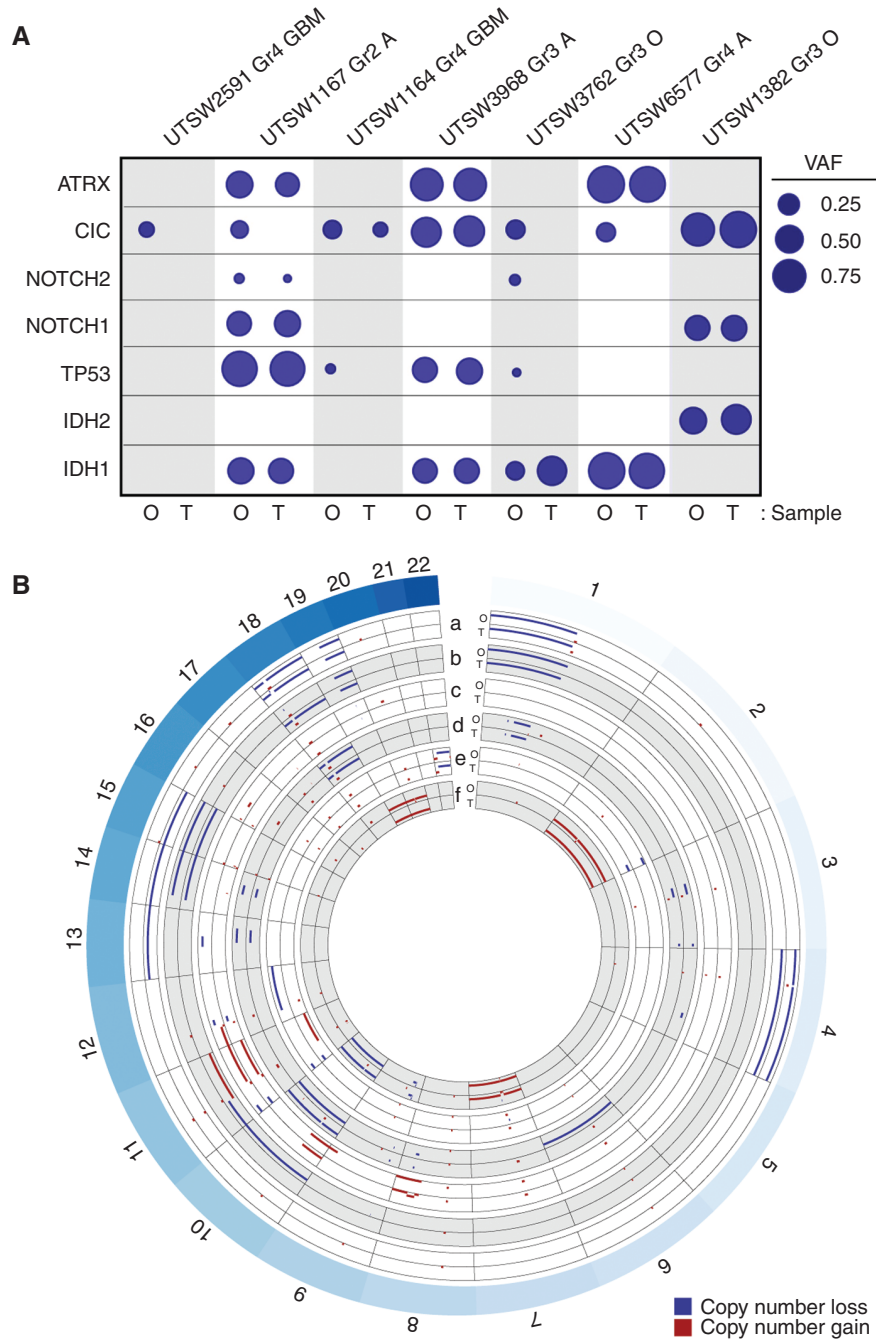
Fig. 5 LGG organoids retain disease-specific genomic hallmarks. (A) LGG organoids largely retain key genetic mutations observed in their respective parental tumor specimens. Genomic DNA from organoid-primary tumor pairs was analyzed via targeted sequencing. Variant allele frequency (VAF) was calculated for each mutated gene. Mutations and single nucleotide variants that are not predicted to be pathogenic were excluded. Circle areas correspond to VAFs for each gene. Abbreviations at top of figure: Gr, Grade; GBM, glioblastoma; O, oligodendroglioma; A, astrocytoma. Abbreviations at bottom of figure: O: organoid, T: tumor. (B) LGG organoids retain copy number alterations observed in their respective parental tumor specimens. DNA sequencing data from part A was used to construct concentric Circos plots depicting copy number variations in paired organoid (O) and tumor (T) samples for the following tumors: a) oligodendroglioma, IDH-mutant, 1p/19q co-deleted, WHO Grade 3 (UTSW1382), b) oligodendroglioma, IDH-mutant, 1p/19q co-deleted, WHO Grade 3 (UTSW3762), c) astrocytoma, IDH-mutant, WHO Grade 3 (UTSW3968), d) GBM, IDH-wildtype, WHO Grade 4 (UTSW1164), e) astrocytoma, IDH-mutant, WHO Grade 2 (UTSW1167), f) GBM, IDH-wildtype, WHO Grade 4 (UTSW2591). Labels around circumference represent chromosome numbers. Scale of each axis ranges from copy number 0 (closer to exterior of the circle) to 4 (closer to interior of the circle), with any regions of copy number 2 not plotted. Red = gains, blue = losses. All samples with copy number >4 are plotted with copy number set to 4. Notably, 1p/19q co-deletion is observed in both organoid and primary tumor samples in a and b. Organoids were cultured for 4–6 weeks after explantation.

longstanding challenge.[30] Tumor cell behavior in the central nervous system is dictated by a diverse set of interactions with other elements of the microenvironment,[31] including signaling and metabolic crosstalk with tumor-resident stromal and immune cells, local fluctuations in nutrient availability, and engagement with structural components of the tumor bed.[32–34] These factors drive epigenetic alterations within gliomas and govern dynamic cellular transitions between canonical transcriptional phenotypes.[35] Therefore, the tumor microenvironment plays a central role in establishing glioma-specific phenotypes and shaping responses to therapy. Substantial progress has been made in recreating the glioma microenvironment in both in vitro and in vivo settings through the development of HGG organoid models[10] and advanced patient-derived and genetically engineered glioma mouse models,[36] respectively. Although in vivo models offer clear advantages in this regard, in vitro models are inherently high-throughput, more tractable to modify and manipulate, and cost-effective.[37] Our study demonstrates that non-tumor stromal cells, including macrophages/microglia and vascular endothelial cells, persist in LGG organoid models, and that these cultures retain cytoarchitectural and gross morphological hallmarks of parental tumors. Therefore, patient-derived LGG organoids present a new platform to study how microenvironmental factors and tumor-stroma interactions impact tumor cell biology in this disease.

Although our study represents, to the best of our knowledge, the first report of in vitro LGG models that maintain relevant microenvironmental features during prolonged culture, we acknowledge that there are limitations to our approach. We collected a relatively small sample set of 22 consecutive tumors at a single academic medical center. Although success rates of organoid origination were uniform, variations in neurosurgical techniques used to acquire tissue specimens and/or intertumoral heterogeneity may modify success rates in other centers and laboratories. Neurosurgical acquisition of these specimens should focus on limiting thermal and mechanical disruption of glioma tissue during microsurgical resection, as even minor damage to glioma tissue may limit the ability to establish these organoids in culture. This study is largely descriptive, demonstrating a method for in vitro perpetuation of LGG tumors, and is not powered for comparative analysis between various methods or treatments. Despite these limitations, our findings lay the groundwork for future studies that leverage this unique organoid modeling approach for evaluation of novel therapeutics and the LGG tumor microenvironment.

Supplementary Material

Supplementary material is available at *Neuro-Oncology* online.

Keywords

glioma | glioblastoma | lower grade glioma | organoids | preclinical models

References

1. Ostrom QT, Gittleman H, Liao P, et al. CBTRUS statistical report: primary brain and central nervous system tumors diagnosed in the United States in 2007-2011. *Neuro Oncol.* 2014;16 Suppl 4:iv1–63.

2. Aldape K, Zadeh G, Mansouri S, Reifenberger G, von Deimling A. Glioblastoma: pathology, molecular mechanisms and markers. *Acta Neuropathol.* 2015;129(6):829–848.

3. Hottinger AF, Abdullah KG, Stupp R. Current standards of care in glioblastoma therapy. In: *Glioblastoma.* Elsevier Inc.; 2016:73–80. doi:10.1016/B978-0-323-47660-7.00006-9

4. Post GR, Dawson G. Characterization of a cell line derived from a human oligodendroglioma. *Mol Chem Neuropathol.* 1992;16(3):303–317.

5. Koivunen P, Lee S, Duncan CG, et al. Transformation by the (R)-enantiomer of 2-hydroxyglutarate linked to EGLN activation. *Nature.* 2012;483(7390):484–488.

6. Kelly JJ, Blough MD, Stechishin OD, et al. Oligodendroglioma cell lines containing t(1;19)(q10;p10). *Neuro Oncol.* 2010;12(7):745–755.

7. Luchman HA, Stechishin OD, Dang NH, et al. An in vivo patient-derived model of endogenous IDH1-mutant glioma. *Neuro Oncol.* 2012;14(2):184–191.

8. Rohle D, Popovici-Muller J, Palaskas N, et al. An inhibitor of mutant IDH1 delays growth and promotes differentiation of glioma cells. *Science.* 2013;340(6132):626–630.

9. Jones LE, Hilz S, Grimmer MR, et al. Patient-derived cells from recurrent tumors that model the evolution of IDH-mutant glioma. *Neurooncol Adv.* 2020;2(1):vdaa088.

10. Pernik MN, Bird CE, Traylor JI, et al. Patient-derived cancer organoids for precision oncology treatment. *J Personal Med.* 2021;11(5):423.

11. Rosenbluth JM, Schackmann RCJ, Gray GK, et al. Organoid cultures from normal and cancer-prone human breast tissues preserve complex epithelial lineages. *Nat Commun.* 2020;11(1):1711.

12. Walsh AJ, Cook RS, Skala MC. Functional optical imaging of primary human tumor organoids: development of a personalized drug screen. *J Nucl Med.* 2017;58(9):1367–1372.

13. Jacob F, Salinas RD, Zhang DY, et al. A patient-derived glioblastoma organoid model and biobank recapitulates inter- and intra-tumoral heterogeneity. *Cell.* 2020;180(1):188–204.e22.

14. Shi Y, Lim SK, Liang Q, et al. Gboxin is an oxidative phosphorylation inhibitor that targets glioblastoma. *Nature.* 2019;567(7748):341–346.

15. Jagannathan L, Cuddapah S, Costa M. Oxidative stress under ambient and physiological oxygen tension in tissue culture. *Curr Pharmacol Rep.* 2016;2(2):64–72.

16. Heddleston JM, Li Z, McLendon RE, Hjelmeland AB, Rich JN. The hypoxic microenvironment maintains glioblastoma stem cells and promotes reprogramming towards a cancer stem cell phenotype. *Cell Cycle.* 2009;8(20):3274–3284.

17. Li Z, Bao S, Wu Q, et al. Hypoxia-inducible factors regulate tumorigenic capacity of glioma stem cells. *Cancer Cell.* 2009;15(6):501–513.

18. Carreau A, El Hafny-Rahbi B, Matejuk A, Grillon C, Kieda C. Why is the partial oxygen pressure of human tissues a crucial parameter? Small molecules and hypoxia. *J Cell Mol Med.* 2011;15(6):1239–1253.

19. Shi D, Wang A, Gao W, et al. Tmod-14. Creation of a genetically engineered mouse model of anaplastic astrocytoma driven by the Idh1-R132h oncogene. *Neuro Oncol.* 2020;22(Supplement_2):ii230–ii231.

20. Louis DN, Perry A, Wesseling P, et al. The 2021 WHO classification of tumors of the central nervous system: a summary. *Neuro Oncol.* 2021;23(8):1231–1251.

21. Philip B, Yu DX, Silvis MR, et al. Mutant IDH1 promotes glioma formation in vivo. *Cell Rep.* 2018;23(5):1553–1564.

22. Dang L, White DW, Gross S, et al. Cancer-associated IDH1 mutations produce 2-hydroxyglutarate. *Nature.* 2009;462(7274):739–744.

23. Losman JA, Kaelin WG Jr. What a difference a hydroxyl makes: mutant IDH, (R)-2-hydroxyglutarate, and cancer. *Genes Dev.* 2013;27(8):836–852.

24. Wakimoto H, Tanaka S, Curry WT, et al. Targetable signaling pathway mutations are associated with malignant phenotype in IDH-mutant gliomas. *Clin Cancer Res.* 2014;20(11):2898–2909.

25. Kumar A, Boyle EA, Tokita M, et al. Deep sequencing of multiple regions of glial tumors reveals spatial heterogeneity for mutations in clinically relevant genes. *Genome Biol.* 2014;15(12):530.

26. Liu X, Ory V, Chapman S, et al. ROCK inhibitor and feeder cells induce the conditional reprogramming of epithelial cells. *Am J Pathol.* 2012;180(2):599–607.

27. Yuan M, White D, Resar L, et al. Conditional reprogramming culture conditions facilitate growth of lower-grade glioma models. *Neuro Oncol.* 2021;23(5):770–782.

28. Blouw B, Song H, Tihan T, et al. The hypoxic response of tumors is dependent on their microenvironment. *Cancer Cell.* 2003;4(2):133–146.

29. McBrayer SK, Mayers JR, DiNatale GJ, et al. Transaminase inhibition by 2-hydroxyglutarate impairs glutamate biosynthesis and redox homeostasis in glioma. *Cell.* 2018;175(1):101–116.e25.

30. Gómez-Oliva R, Domínguez-García S, Carrascal L, et al. Evolution of experimental models in the study of glioblastoma: toward finding efficient treatments. *Front Oncol.* 2020;10:614295.

31. Srinivasan ES, Tan AC, Anders CK, et al. Salting the soil: targeting the microenvironment of brain metastases. *Mol Cancer Ther.* 2021;20(3):455–466.

32. Parsons DW, Jones S, Zhang X, et al. An integrated genomic analysis of human glioblastoma multiforme. *Science.* 2008;321(5897):1807–1812.

33. Quail DF, Joyce JA. The microenvironmental landscape of brain tumors. *Cancer Cell.* 2017;31(3):326–341.

34. Bi J, Chowdhry S, Wu S, Zhang W, Masui K, Mischel PS. Altered cellular metabolism in gliomas - an emerging landscape of actionable co-dependency targets. *Nat Rev Cancer.* 2020;20(1):57–70.

35. Wang Q, Hu B, Hu X, et al. Tumor evolution of glioma-intrinsic gene expression subtypes associates with immunological changes in the microenvironment. *Cancer Cell.* 2017;32(1):42–56.e6.

36. Hicks WH, Bird CE, Traylor JI, et al. Contemporary mouse models in glioma research. *Cells.* 2021;10(3):712.

37. da Hora CC, Schweiger MW, Wurdinger T, et al. Patient-derived glioma models: from patients to dish to animals. *Cells.* 2019;8(10):1177.